https://dx.doi.org/10.4314/dujopas.v9i4a.26
ISSN (Print): 2476-8316
ISSN (Online): 2635-3490
Dutse Journal of Pure and Applied Sciences (DUJOPAS), *Vol. 9 No. 4a December 2023*

Aeromagnetic Data Investigation of Geothermal Energy Potentials in Ramfashi and Environs Zamfara State, Nigeria

Kamureyina Ezekiel[1], Sarah Peter[1] Mohammed Ali Garba[2]

[1]Department of Geology,
Adamawa State University,
P.M.B. 25, Mubi
Nigeria

[2]Department of Geology,
Gombe State University.
P.M.B.127, Tudun Wanda
Gombe,
Nigeria.

Email: kamureyina123@gmail.com

Abstract

The goal of the geothermal study over Ramfashi and Environs in Northwestern Nigeria was to use aeromagnetic data to determine the region's heat flow, geothermal gradient, and Curie point depth. For the purpose of analyzing the aeromagnetic data, on residual and regional magnetic intensity were gathered using regional residual separation. The residual data was upward continuued to obtain the upward data to perform spectral analysis. This allowed for calculation of depths to centroid and top boundary, which in turn allowed for calculation of region's heat flow, geothermal gradient, and Curie point. The analysis's conclusions revealed that, with an average value of 48.53 °Ckm^{-1}, the distances to the heat flow, top boundary, centroid, and Curie point varied between 6.73 km and 7.39 km, 2.01 km and 2.16 km, and 113.55 mWm^{-2} and 128 mWm^{-2} respectively. Geothermal gradient also varied between 45.42 °Ckm^{-1} and 51.33 °Ckm^{-1}. According to the heat flow data from this investigation, the area possesses anomalous geothermal energy and a sizable heat source.

Keywords: Geothermal gradient, Heat flow, Ramfashi, Curie-point, Aeromagnetic data

INTRODUCTION

The energy produced and stored on Earth is known as geothermal energy. This power may be studied using different methods to determine the heat flow, Curie point depth, and geothermal gradient of a place. The earth's temperature rises per unit depth as a result of heat escaping from the center is known as the geothermal gradient. Distribution of subsurface temperature can be accurately predicted using geothermal gradients. Elmasry *et al*. (2022) state that one of the measures used in understanding geothermal gradient is through geophysical well logging, which is crucial for understanding sub- and regional-scale tectonics. It is helpful in determining a region's potential for geothermal resource development as well (Ciriaco *et al.*, 2020).

**Author for Correspondence*

Matter's temperature is determined by thermal energy. The planet's creation, radioactive mineral decay, volcanic activity, and solar radiation received at the surface are the sources of Earth's geothermal energy. Geothermal energy has historically only been available in regions close to tectonic plate borders, despite being economical, dependable, sustainable, and environmentally benign. Accordingly, it is anticipated that regions with geothermally active soils would have shallow Curie point depths (Yakubu *et al*., 2023; Alkali *et al*., 2023). Furthermore, most of the surface-visible geodynamic processes are directly regulated by the earth's interior temperature (Geng *et al*., 2023).

The purpose of this research is to provide clues to likely productive zones for geothermal exploitation. Nigeria's chronic power supply problems, which have existed for some time, could be resolved if geothermal energy is properly utilized. Besides, Renewable energy is the safest and healthiest energy that our country Nigeria requires for the progress and development of the Nation.

The research area, which includes portions of the Zamfara State, is situated within longitudes 5° N and 6° N, latitudes 11°30E and 12°30'E (Figure 1). It has a lateral extent of 109km x 109km totaling an area of approximately 12056.04km^2. The research region is in northwest Nigeria's Sokoto basin. It can be accessed by linking trails and the primary roads in the area. Physiographic and climatic features of the area under study include temperature, rainfall, and land forms and drainage. The topography and landforms of the area are generally lowland with an undulating plain (Figure 1).

There is a dendritic drainage pattern in the region. The Zamfara River is a river that flows across the northern region of Nigeria; it rises in Zamfara State and flows west into Kebbi State, where it meets the Sokoto River before flowing southwest to Birnin Kebbi. The river also flows southwest and eastward. The temperature in the research location is characteristic of the savannah climate of West Africa's Sokoto basin. One of Nigeria's warmest locations is the Sokoto basin, which is situated in the Sahel region of Africa (Akudo and Otaru, 2023; Ilesanmi, 2023). Therefore, Zamfara has a dry and wet type of climate. Rainy season last from May to September, with dry season prolonging from October to April (Abubakar *et al*., 2023; Usman *et al*., 2023), when dusty harmattan winds from the northeast predominate.

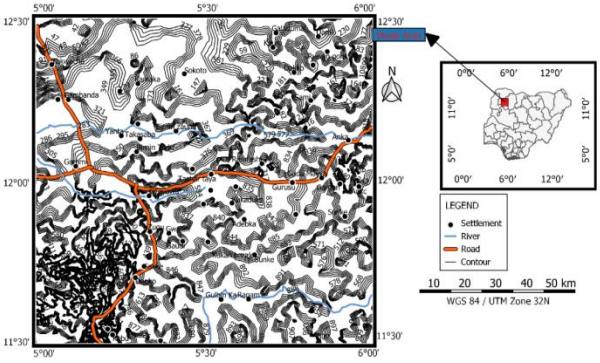

Figure 1: A topographic research area map (updated in 2006 using the digital elevation model).

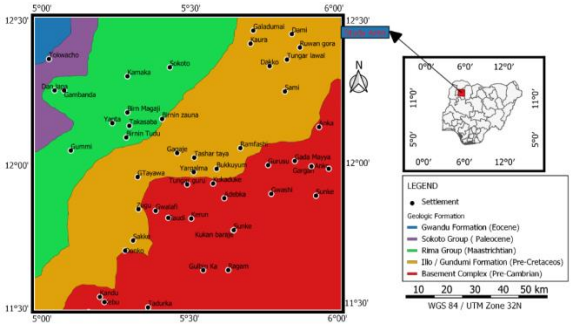

Figure 2: Study area Geologic map (Adapted from Nigerian Geological Survey Agency,2006)

Geology of the Study Area

The Basin in northwest Nigeria (Figure 2) is a portion of the Iullemmeden basin's South Eastern region. The Basin is a young (Tertiary–Mesozoic) inland Cratonic sedimentary basin located in West Africa. The basin formed by epierogenic warping of stretching and rifting of

technically stabilized crust, similar to more intracontinental basins in the region, as well as the continent of Africa overall (Tawey *et al*., 2023). The sediments were deposited over the Precambrian Basement unconformable throughout four primary stages of deposition, based on the research area map. This include, Illo/Gundumi Formation, Rima Group, Sokoto Group, and Gwandu Formation.

The Basement complex is a component of the Pan-African mobile belt, which form as a result of plate collision between the active Pharusian continental margin and the passive continental margin of the West African Craton. The Nigerian basement was reactivated and was impacted by the 600 million year Pan African orogeny (Alkali *et al*., 2023). The Liberian (2,700 Ma), Kibaran (1,100 Ma), and Pan-African (600 Ma) Orogenic cycles are thought to have produced at least four main Orogenic cycles of deformation, metamorphism, and remobilization, which are represented by the basement rocks.

The lacustrine and fluviatile Pre-Maastrichtian "Continental Intercalaire" of West Africa includes the grit-and-clay Illo/Gundumi formation. Conversely, the lateral counterpart, the Illo Formation, is mostly composed of sandstone, cross-bedded pebbly grits, and pisolite clay, which is recognized for its high bauxite content. Gundumi is only crossed by the Rima Group (Abubakar *et al*., 2023).

The Group is made up of the Maastrichtian mudstones and friable sandstones of Taloka and Wurno Formations divided by the fossiliferous, calcareous, and shaley Dukamaje Formation (Lawal *et al*., 2023). The oldest of the three formations, of which the Taloka Formation is composed some carbonaceous mudstone, poorly reddish-purple to brown siltstones that have been cemented, and white, fine-friable sandstone (Lawal *et al*., 2023). The main constituents of the Dukamaje fossiliferous gypsiferous shale with some marl-mudstone in the formation intercalations and a distinctive bone bed near the base. The Wurno Formation is the youngest. According to Phillips *et al*. (2023) it shares lithologic connections with the Taloka Formation. It is made up of siltstone, intercalated mudstones, and pale, friable, fine-grained sandstone (Abubakar *et al*., 2023).

With the Gamba Formation included, the Sokoto Group is composed primarily of shales divided by the calcareous Kalambaina Formation (Abubakar *et al*., 2023). Kalambaina Formation consists of light grey and white grey clayey limestone, nodular and crystalline. According to Emmanuel *et al*. (2020), the lithological unit of the formation is made up of calcareous beds and an upper laterite cover that were buried beneath the limestone series. The Sokoto Formation Group's bottom unit is called the Dange Formation. It is located above the Wurno and is mostly made up of thin strata of limestone and marl units interbedded with yellowish to greenish-grey marine clay shale.

Gwandu Formation (Eocene Continental Terminal) lies uncomfortably on the Kalambaina Formation. It is Eocene and the youngest Tertiary formation in the basin. The partially solidified sands and clays, with a continental origin, were interbedded. The thick, huge clay beds are colored black, brown, red, white, and grey. There is fine to extremely coarse sand. The formation also contains lignite beds. The younger alluvial covers the Gwandu Formation and is primarily found along the River Sokoto and its tributaries (Arogundade *et al*., 2023).

MATERIALS AND METHODS

Data Gathering

Aeromagnetic data of total field intensity were used in the investigation. These data from the Nigerian Geological Survey Agency (NGSA) were acquired by Fugro Aerial Survey Company used who used magnetometer with 3X Scintrex CS3 Cesium Vapour, line spacing of 500 meters, NW-SE direction, height of 80 meters, and tie distance of 2 kilometers to collect the data as part of a program to support and promote mineral exploration in Nigeria in 2009.

Methods of Processing of Aeromagnetic Data

The aeromagnetic data was filtered using several combinations of filters in order to disclose specific elements that supported the interpretation. The system was therefore fed with the digital data to provide the comprehensive map of magnetic intensity. depth to the centroid (Z_o), depth to the boundary (Z_t), and regional and residual maps were obtained by applying high-resolution filtering techniques to the Total Magnetic data, including upward continuation, spectrum analysis, geothermal gradient, curie point and heat flow.

Separation of Regional Residuals

This was performed using the polynomial fitting method to produce the residual map. The process is based on the statistical theory, and residual features exposed as random errors by matching with a low-order mathematical polynomial (Florio *et al*., 2023). The mathematically characterized surface with the closest possible fit to the magnetic field within a predetermined level of detail is computed using the observed data, typically using the least squares approach. Residual is the difference between the magnetic field value that was computed using this surface (Onwubuariri *et al*., 2023; Akintoye *et al*., 2023). Using the polynomial fitting method, the regional field was subtracted from the total magnetic field to create the residual magnetic field of the research area.

Upward Continuation

By reducing the effects caused by local features, the upward continuation was utilized to make the emergence of regional magnetic anomalies more straightforward. Regional features are frequently hidden by the abundance of local magnetic anomalies. Thus, these disruptions were smoothed out by upward continuation without affecting the primary regional traits. Viewing the strength of the magnetic field above the level of flight is the primary goal of upward continuation, which aims to reduce by emphasizing longer wavelength anomalies that represent regional features instead of shorter ones (Ayua *et al*., 2023; Cho and Janda, 2023) The following is the equation for upward continuation:

$$F\,x, y, -h = h\,2\pi \int f\,x, y, o\,\partial x\,\partial y\,x-x'\,2+\,y-y'\,2+h^2)\,½ \quad (1)$$

Where F x′, y′, −h = total field at a point

F x′, y′, −h above the surface on which F x′, y′, −0 is known.

h = continuation height.

The upward continued map was made using the residual map that was upward continued to a distance of three kilometers. Oasis Montaj and Matlab software were used to do spectrum analysis on the upward-continued information to determine the depth of the Curie point. This made it possible for us to calculate depths of Top Boundary to the Centroid. The data was split up into four (4) 30-by-30-foot sections. Using Oasis Montaj software, the radially average power spectrum of each block was obtained by applying Fast Fourier transfer. It was then imported to Excel where it was converted to a format acceptable by Mat lab, where the slope of best filing points was drawn to obtain Z_o and Z_t. values.

Depth of Curie Point

The calculation of Curie point depth took two phases (Tarshan *et al*., 2023): The slope of the longest wave length spectrum is used to calculate the distance to the centroid (Z_o) of the magnetic source.

In [p s1/2] = InA-2/s/Zo (2)

where p(s) is the radially averaged power spectrum of the anomaly and s is the wave number. and A is a constant. The depth to the top border (Z_t) of the magnetic source was estimated in the second step using the slope of the line with the second wavelength.

$\log \{P(K)^{1/2}\} = logB - 2\pi/s/Z_t \ \ k$ (3)

where B is a sum of constants independent of K.

The magnetic source's basal depth (Z_b) was then calculated using the following equation:

$Z_b = 2Z_o - Z_t$ (4)

It is expected that a magnetic source's acquired basal depth (Z_b) equals the depth of its Curie point (Ezeh and Magbo, 2023).

Heat flow and Geothermal gradient

It (Heat flow) refers to circulation of heat, from interior of earth to the exterior (Abdullahi *et al*., 2023; Barka and Nur, 2023; Yaro *et al*., 2023).

Using Fourier's Law, the following formula was employed to calculate the thermal gradient and heat flow. (Nika, 2023).

$Q=\lambda[\partial T/\partial Z]$ (5)

the heat flow Q is.

Temperature gradient dT/dZ and vertical direction of temperature variation are both considered to be constant in this equation. The following equation defined the geothermal gradient ($\partial T/\partial Z$) between the earth and the Curie point depth (Z_b):

$\frac{\partial T}{\partial Z} = \frac{580°C}{Z_b}$ (6)

Additionally, the formula below was used to link the heat flow to the geothermal gradient (q):

$Q = \lambda(\frac{\partial T}{\partial Z}) = \lambda(\frac{580°C}{Z_b})$ (7)

Where the heat conductivity coefficient, represented by λ,

The magnetic mineralogy affects the Curie temperature.

Eigenmal conductivity (λ) is taken to be constant when computing the temperature distribution in the crust, and it ranges from 2 to 4$mWm^{-1}°C^{-1}$ (Zhang *et al*., 2023; Yakubu *et al*., 2023). 2.5 $mWm^{-1}°C^{-1}$ was selected as the thermal conductivity for this experiment.

RESULTS

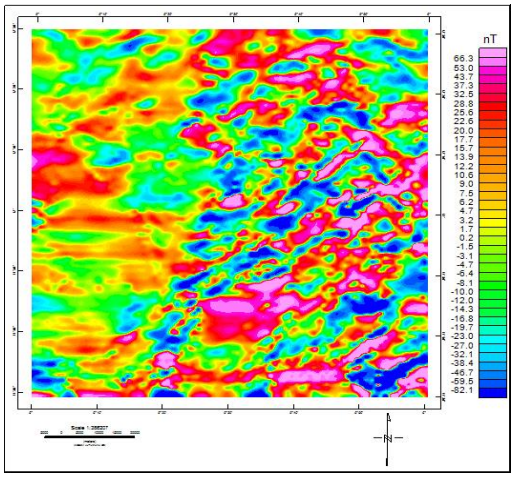

Figure 3: A map showing the study area's total magnetic intensity.

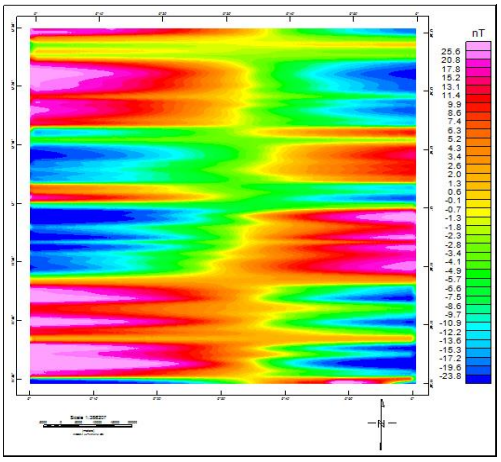

Figure 4: A regional magnetic map of research area

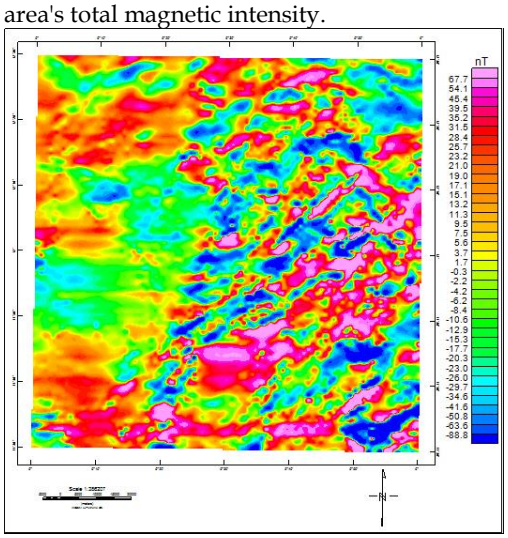

Figure 5: Map of the Study Area's Residual Magnetic Intensity

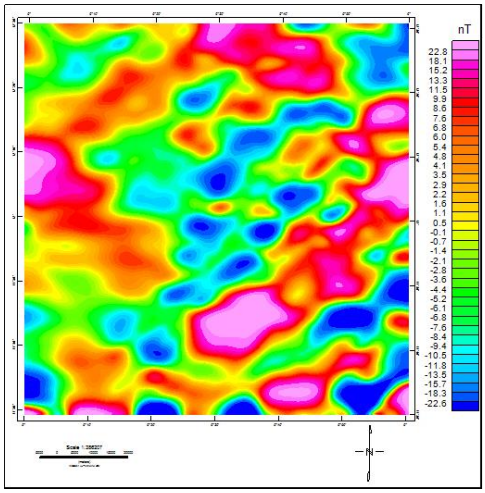

Figure 6: Upward Continuation of the Study Area Map.

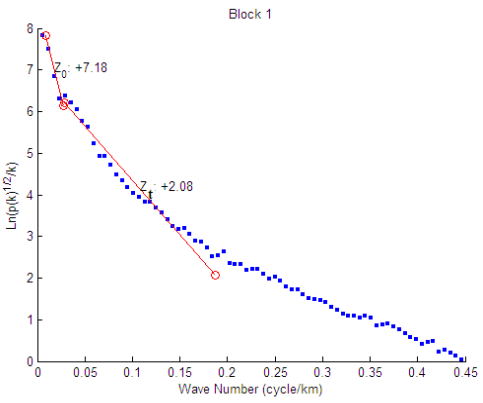

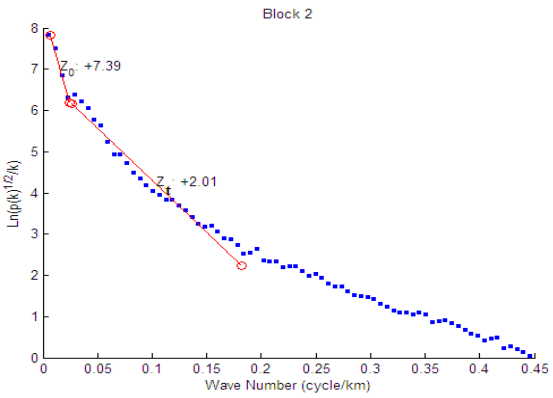

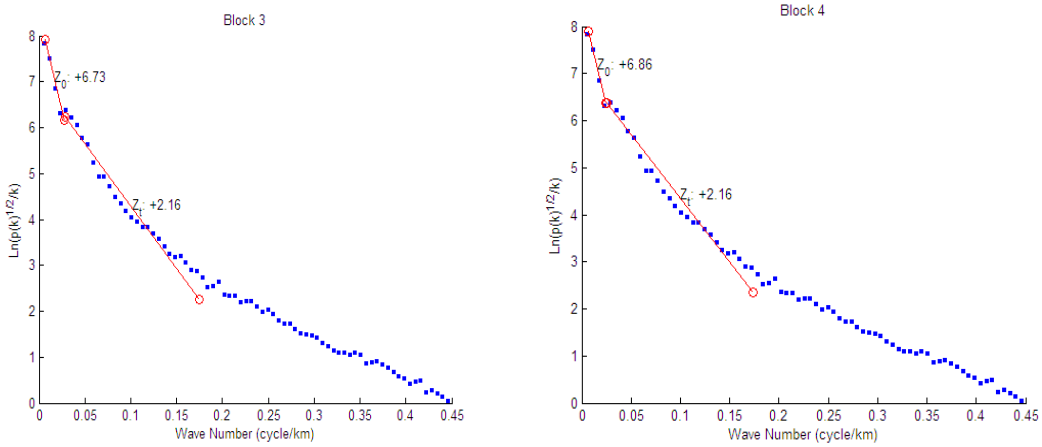

Figure 7: Graphs of Spectral Blocks 1 to 4 of the study area.

Table 2: Calculated Curie Point Depth, Geothermal Gradient, and Heat Flow.

Blocks	Z_o (km)	Z_t (km)	Z_b (km)	$\left[\frac{\partial T}{\partial z}\right]$ °Ckm $^{-1}$	Q(mWm^{-2})
1	7.18	2.08	12.28	47.23	118.07
2	7.39	2.01	12.77	45.41	113.55
3	6.73	2.16	11.30	51.32	128.33
4	6.86	2.16	11.56	50.17	125.42
Total	28.16	8.41	47.91	194.13	485.37
Average	7.04	2.1025	11.9775	48.5325	121.3425

DISCUSSION

The research area's complete magnetic intensity map (Figure 3) extends from -82.1nT to 66.3nT. The An analysis of the anomalies included in the total magnetic intensity map visually indicates that most of them are trending in the NE-SW, NW-SE, and E-W directions. The blue color anomalies range from -82.1nT to -16.8nT, the green color anomalies range from -14.3nT to -1.5nT, the yellow color anomalies range from 0.2nT to 13.9nT, red color anomalies range from 15.7nT to 25.6nT and the pink color anomalies from 28.8nT to 66.3nT.

The regional magnetic intensity map (Figure. 4) varies from -23.8nT to 25.6nT. The lowest regional magnetic intensity map is -23.8nT and the highest value of 25.6nT. the blue anomalies vary from -22.6nT to -8.4nT, green anomaly vary from -7.6nT to -1.4nT, the yellow anomaly vary from -0.7nT to 6.0nT, the red anomaly vary from 6.6nT to 11.5nT and the pink color anomaly vary from 13.3nT to 22.8nT. The anomalies trend from East to West.

A high magnetic value of 22.8 nT and a low magnetic value of -22.6 nT are displayed on the study area's Map of magnetic intensity residuals (Figure 5). The degree to which the magnetic green color anomalies ranges from -6.8nT to -1.4nT, trending from NE-SE, SW-NW directions, and dominating almost the entire map. The pink color anomalies range from 11.5nT to 22.8nT, and they are prominent in the NE, SE, and East, as well as small pockets in the SSW and WNW. The red color anomalies range from 6.0nT to 9.9nT and they occur around the pink color anomalies. The yellow color anomalies range from -0.7nT to 5.4nT. The blue color anomalies range from -22.6nT to -7.6nT which are present in the NE-SE, NNE, ESE, SSW, and SW with smaller pockets in the NW directions and are dominant in the center of the map.

The upward continuing map (Figure 6), which was produced using the residual magnetic map, exhibits the same pattern of anomalies as the residual map, with the maximum magnetic

intensity being 67.7nT and the lowest being -88.8nT. Similar to the residual magnetic map, the map exhibits blue, green, yellow, red, and pink color anomalies. Red color anomalies range from 21.0nT to 35.2nT, pink color anomalies from 39.5nT to 67.7nT, green color anomalies from -0.3nT to -17.7nT, yellow color anomalies from 15.1nT to 19.0nT, and blue color anomalies from -88.8nT to -20.3nT. Contrary to the residual map, the anomalies are more obvious as a result of the suppression of near-surface anomalies, which enhances the deeper anomalies. Figure 7 demonstrates how the logarithms of spectral energy against frequencies are constructed for every block.

Two linear segments were taken out of every graph. From the slope of the second longest wavelength segment, the boundary Z_t of that distribution was computed. These lengths with a mean value of 7.04 km and 2.1025 km, respectively, and vary from 6.73 km to 7.39 km and 2.01 km to 2.16 km, respectively. It was determined how centroid Z_o of the magnetic source was from slope of longest wavelength segment. Table 2 provides an overview of the depths (Z_o and Z_t) used to calculate the heat flow, Curie point depth, and geothermal gradient. Curie point depth is the temperature below each block at which magnetic elements start to lose their characteristics. The average Curie point depth in the research region was found to be 11.98 km, with a range of 11.30 km to 12.77 km. The Curie point result is consistent with that of Alkali *et al*. (2023), who hypothesized that a curie point isotherm with a length ranging from 11.36 km to 22.30 km lies beneath the Sokoto basin. Nwonko (2017), who conducted research across the Nupe basin in North Central Nigeria between longitude 4°00'' and 6°00''E and latitudes 8°30'' to 10°00'N, demonstrated that there is a 12–13 kilometer variation in the curie point depth.

Geothermal gradients are defined as temperature increases with depth. By using the curie temperature of 580°C and the expected Curie point depths, the geothermal gradient has an average value of 48.53°Ckm^{-1} and ranges from 45.41°Ckm^{-1} to 51.32°Ckm^{-1}. The curie point, which symbolizes the Heat is transferred from the earth's interior to its surface. temperature at which magnetic materials become paramagnetic and lose their magnetic properties. The curie point depth and the geothermal gradient are inversely correlated. Suleiman (2012) recorded temperatures ranging from 30.61°Ckm^{-1} to 58.37°Ckm^{-1}. whereas Nwankwo and Shehu (2015) acquired geothermal gradients between 20.84°Ckm^{-1} and 52.11°Ckm^{-1}. These results are comparable to those of previous investigations regarding geothermal gradient results. Averaging 48.5325 mWm^{-2}, heat flow of the area ranges from 113.55mWm^{-2} to 128.33 mWm^{-2}. Underneath thick strata of the area, igneous intrusion may have caused this. Thermally stable continental regions are said to have average heat flows of more than 60 mWm^{-2}. However, values between 80 mWm^{-2} and 100 mWm^{-2} are considered to be a decent geothermal reservoir, and values above 100 mWm^{-2} are an indication of an exceptional geothermal condition, according to Ofor and Udensi (2014); Nwankwo and Shehu (2015); Ezekiel (2019). Geological factors affect Curie point depth, geothermal gradient, and heat flow (Ofor and Udensi, 2014). Since volcanic and metamorphic zones have heat conductivities, they typically have substantial heat flow. Geothermal studies focus on the earth's heat, which is heat that is moving from the planet's interior to the surface. Magma and radioactive sources are the two most common types of sources of heat in the natural world. Other sources of heat emitted during the Earth's spin-axis tidal force and electromagnetic influences of the Earth's magnetic field include as follows (Nwankwo and Shehu, 2015). The earth's evolution reflects the history of heat transmission from the interior. The primary directly observable quantity for heat flow is the temperature gradient close to the surface, which is utilized to compute the flow of heat from the interior and subsequently draw conclusions about the thermal structure and evolution. The total magnetic intensity of the research region indicates

a variety of magnetic anomalies that vary from -82.1nT to 66.3nT, while residual magnetic anomaly values range from -23.8nT to 25.6nT. The residual magnetic field highlighted local characteristics that are often obscured by the broad aspects of the regional field. Strong positive anomalies probably point to locations with a larger concentration of magnetically susceptible minerals, whereas broad magnetic lows probably point to areas with a lower proportion of susceptibility minerals. Table 2 shows that related heat flow varies between 118.07mWm^{-2} and 128.33mWm^{-2}, with an average value of 121.34mWm^{-2}, and the geothermal gradient associated with the computed Curie depths from spectral analysis varies between 47.23^{o}Ckm^{-1} and 51.32^{o}Ckm^{-1}, with an average value of 48.53oCkm^{-1}. It has been demonstrated that heat flow rises as Curie point depth decreases. This demonstrated that an anomalously high temperature gradient and heat flow are present at the location of high geothermal energy. As a result, it is expected that places that are geothermally active will be near the Curie point. This result was in good agreement with the results of other researchers that used a curie point temperature of 580°C to compute the curie point depth. The relevant heat flow anomalies in the study area were then identified using the thermal conductivity of 2.5 Wm^{-1}°C^{-1} (Ofor and Udensi, 2014; Nwankwo and Shehu, 2015). Changes in the geothermal gradient in the region were discovered.

The majority of recent literature claims that geological factors have a significant impact on the heat flow and curve-point depth. Heat flow is the main parameter that can be seen in geothermal investigation. Due to the high heat conductivities of volcanic and metamorphic zones, high heat flow values are typically associated with these places. According to literature like Nwankwo and Shehu (2015), the Curie point depth is highly reliant on geological factors. For volcanic and geothermal fields, Curie point depths are less than 15km, between 15 and 25km for island arcs and ridges, and more than 20km for plateaus and trenches.

CONCLUSION

Aeromagnetic anomaly data with high precision over Ramfashi and the neighboring areas in northwest Nigeria were investigated to be able to calculate the geothermal gradient, heat flow, and Curie Point depth for geothermal energy potentials. Based on findings, values above 100mWm^{-2} are indicative of anomalous geothermal conditions, and the study's results indicate that the thermal structure of the crust in this region has a high heat flow value above this recommended range. This range is thought to be a good geothermal reservoir. Based on the results, the research region (average heat flow: 121.3425mWm^{-2}) is indicative of unusual geothermal conditions.

ACKNOWLEDGEMENT

We are appreciative that the aeromagnetic data for the Nigerian Geological Survey Agency was made available.

REFERENCES

Abdullahi, M., Valdon, Y.B., Andrew, F.P. and Idi, B.Y, 2023. Curie Depth and Surface Heat Flow Estimation from Anomalous Magnetic Blocks in the Lower and Part of Middle Benue Trough and Anambra Basin. *Earth and Planetary Science*, *2*(1), pp.11-20.

Abubakar, A., Likkason, O.K., Maigari, A.S. and Ali, S., 2023. Sediment thickness of subsurface anomalous Sources Determined by 2D/3D modeling of Potential field Gravity data: Implications for Sokoto Inland Basin Structures, NW, Nigeria.

Abubakar, I., Bello, B.M., Tukur, K., Maiakwai, N.S. and Sani, M.M., 2023. Checklist, Diversity and Abundance of the Flora in some Selected Local Government of Zamfara State, Northwestern, Nigeria.

Akintoye, G.S., Bassey, N.E. and Udoh, A.C., 2023. Geological Analysis of Gravity Data Over Part of Nigeria's NorthCentral Basement Complex. *Journal of Mining and Geology*, *59*(1), pp.87-98.

Akudo, E.O. and Otaru, P.O., 2023. The influence of climate change on freshwater availability in the Sokoto Rima River Basin, Northwestern Nigeria. *Environmental Monitoring and Assessment*, *195*(1), p.82.

Alkali, A., Alhassan, D.U., Lawrence, J.O., Rafiu, A.A., Adetona, A.A., Salako, K.A. and Udensi, E.E., 2023. Investigating Geothermal Resource Potential in Parts of North Central Nigeria using Aeromagnetic Data. Nigeria Institute of Physics (NIP) 44th Annual Conference Proceedings.

Arogundade, A.B., Ajama, O.D., Ayinde, I.S., Falade, S.C. and Awoyemi, M.O., 2023. Investigation of structural controls on the drainage system of north-western Nigeria. *Acta Geophysica*, *71*(4), pp.1747-1762.

Ayua, K.J., Ugwu, J.U. and Hassan, Y., 2023. Re-evaluation of HRAM data of Gboko and Katsina-ala area for hydrocarbon and solid mineral potential. *World Scientific News*, *178*, pp.56-78.

Barka, J. and Nur, A., 2023. Geothermal prospective areas in the Northern sector of Bida Basin and environs, North-Central Nigeria. *Science World Journal*, *18*(3), pp.509-518.

Cho, J. and Janda, S., 2023. Reciprocity in upward product line extensions: A longitudinal study. *Journal of Retailing and Consumer Services*, *70*, p.103161.

Ciriaco, A.E., Zarrouk, S.J. and Zakeri, G., 2020. Geothermal resource and reserve assessment methodology: Overview, analysis and future directions. *Renewable and Sustainable Energy Reviews*, *119*, p.109515.

Elmasry, A., Abdel Zaher, M., Madani, A. and Nassar, T., 2022. Exploration of Geothermal Resources Utilizing Geophysical and Borehole Data in the Abu Gharadig Basin of Egypt's Northern Western Desert. *Pure and Applied Geophysics*, *179*(12), pp.4503-4520.

Ezeh, C.C. and Magbo, C.J., 2023. Evaluation of Geothermal Energy Potential in Parts of the Lower Benue Trough, Nigeria, Using Aeromagnetic Data. *Journal of Earth Sciences and Geotechnical Engineering*, *13*(2), pp.1-22.

Ezekiel, K., 2019. Geothermal Study over Sokoto Basin Northwestern, Nigeria. *International Journal of Engineering and Science Invention*. 8(5), pp. 34-48.

Florio, G., Fedi, M. and Cella, F., 2023. A fractional vertical derivative technique for regional-residual separation. *Geophysical Journal International*, *232*(1), pp.601-614.

Geng, M., Ali, M.Y., Fairhead, J.D. and Saibi, H., 2023. The Curie depths of the United Arab Emirates: Implications for regional thermal structures and tectonic terranes. *Tectonophysics*, *848*, p.229721.

Ilesanmi, O.A., 2023. Assessing the Impact of Changing Climate on Crop Water Requirements in Nigeria. *Agricultural Engineering International: CIGR Journal*, *25*(3).

Lawal, M., Hassan, M.H.A., Abdullah, W.H. and Otchere, D.A., 2023. Sedimentary facies and stratigraphy of the Campanian-Maastrichtian Taloka Formation, southeastern Iullemmeden Basin, Nigeria. *Journal of African Earth Sciences*, *200*, p.104842.

Nika, G., 2023. A gradient system for a higher-gradient generalization of Fourier's law of heat conduction. *Modern Physics Letters B*, *37*(11), p.2350011.

Nwankwo, l.I. and Shehu, A.T. 2015. Evaluation of Curie point depths, geothermal gradients, and near-surface heat flow from high-resolution (HRAM) data of the entire Sokoto basin, Nigeria, *Journal of Volcanology and Geothermal Research*. 305.pp.45-55.

Nwankwo, l.I., 2017. Spectral Evolution of Aeromagnetic Anomaly map for Geothermal Exploration in the part of Nupe basin, West Central Nigeria. Ph.D. Thesis University of Ilorin.

Ofor, N.P. and Udensi, E.E. 2014. Determination of heat flow in the Sokoto basin, Nigeria using spectral analysis of aeromagnetic data. *Journal of natural science research*. 4(6),pp.83-93.

Onwubuariri, C.N., Nwokoma, E.U., Ezere, U.A., Ugwu, J.U. and Onwudo, C.T., 2023. Geophysical Investigation of Environmental and Engineering Features Using Aeromagnetic Data of Ogoja and Environs Southeastern Nigeria. *The Nigerian Journal of Physics (NJP)*, *32*(1), pp.9-22.

Phillips, O.A., Adebayo, A.J., Abdulganiyu, Y. and Apanpa, K.A., 2023. Geochemical elements as provenance and paleoenvironmental indicators in siliciclastic sediments of Neogene Gwandu formation exposed in Birnin Kebbi Area, Northwestern Nigeria. *Ife Journal of Science*, *25*(2), pp.217-237.

Tarshan, A., Azzazy, A.A., Mostafa, A.M. and Elhusseiny, A.A., 2023. Determination of Curie Point Depth and Heat Flow Using Airborne Magnetic Data over the Kom-Ombo and Nuqra Basins, Southern Eastern Desert, Egypt. *Geomaterials*, *13*(4), pp.91-108.

Tawey, M.D., Adesoji, I.A. and Oziofu, E.A., 2023. Comparative Depth to Magnetic Source Analysis of Shanga (Sheet 96), Northwestern Nigeria Using Aeromagnetic Data. *African Journal of Environmental Sciences and Renewable Energy*, *12*(1), pp.56-69.

Tijani, M.N., 2023. Geology of Nigeria. In *Landscapes and Landforms of Nigeria* (pp. 3-32). Cham: Springer Nature Switzerland.

Usman, S.U., Umar, N. and Abdulhamid, A.I., 2023. Climate Change and Drought in the Dryland Areas of Nigeria. In *Climate Change Impacts on Nigeria: Environment and Sustainable Development* (pp. 361-378). Cham: Springer International Publishing.

Yakubu, J.A., Amuche, I.D., Igwe, A.E., Shuaibu, A. and Okwesili, A.N., 2023. Investigation of Curie Point Depth Using High Resolution Aeromagnetic of Igumale and Ejekwe Area, Lower Benue Trough Nigeria. *Indian Journal of Science and Technology*, *16*(8), pp.540-546.

Yaro, U.Y., Abir, I.A. and Balarabe, B., 2023. Determination of Curie point depth, heat flow, and geothermal gradient to infer the regional thermal structure beneath the Malay Peninsula using de-fractal method. *Arabian Journal of Geosciences*, *16*(1), p.84.

Zhang, L., Cao, Z., Fu, Q.Q., Li, C.Y., Du, Y.Q., Li, Y.N., La, T., Zhang, D.B. and Wang, J., 2023. Thermoelectric properties of Yb-La-Nb-doped SrTiO3. *Journal of the European Ceramic Society*.